

2016

Falling Film Evaporation On A Thermal Spray Metal Coated Vertical Corrugated Plate Conduits

Jerin Robins Ebenezar

Indian Institute Of Technology Madras, India, jerinre@gmail.com

Annamalai Mani

Indian Institute Of Technology Madras, India, mania@iitm.ac.in

Follow this and additional works at: <http://docs.lib.purdue.edu/iracc>

Ebenezar, Jerin Robins and Mani, Annamalai, "Falling Film Evaporation On A Thermal Spray Metal Coated Vertical Corrugated Plate Conduits" (2016). *International Refrigeration and Air Conditioning Conference*. Paper 1575.
<http://docs.lib.purdue.edu/iracc/1575>

This document has been made available through Purdue e-Pubs, a service of the Purdue University Libraries. Please contact epubs@purdue.edu for additional information.

Complete proceedings may be acquired in print and on CD-ROM directly from the Ray W. Herrick Laboratories at <https://engineering.purdue.edu/Herrick/Events/orderlit.html>

Falling film evaporation on a thermal spray metal coated vertical corrugated plate conduits

Jerin Robins EBANESAR, Annamalai MANI*

Indian Institute of Technology Madras, Department of Mechanical Engineering,
Chennai, India

* Corresponding Author: mania@iitm.ac.in, +91 44 22574666

ABSTRACT

In falling film evaporation process, the heat is transferred from the condensing fluid to the liquid flowing over it. Tube geometry and tube size have an important role on the performance of the falling film evaporators. This paper presents a two dimensional CFD study of water falling film evaporation on a thermal spray metal coated vertical corrugated conduits. Two-phase flow simulation is done by using a finite volume method based commercial software, using $k-\omega$ equations with shear stress transport (SST). Sinusoidal corrugations with different porosity have been selected for the study. Evaporation and heat transfer during falling film evaporation are included through user defined functions (UDFs). Effect of Reynolds number, wall superheat and surface roughness on heat transfer coefficient is presented. Numerical results are compared with the results of horizontal circular tube falling film evaporation from literature. An enhancement of film heat transfer coefficient of at least 15% is observed for the vertical corrugated plate conduits.

Key words

Falling film evaporation, vertical corrugated plate conduit, numerical simulation, heat transfer enhancement, thermal spray metal coating

1. INTRODUCTION

Horizontal shell-side falling film evaporators have a significant potential to replace flooded evaporators. Compared to flooded type evaporators, falling film evaporators need less working fluid and its small pressure drop and higher heat transfer coefficient will make the falling film evaporators dominate over the conventional flooded type evaporators. But, due to shell and tube configuration, the falling film evaporators are bulky like flooded tube evaporators. Another, main problem concerning about the film evaporation over horizontal tubes are the formation of dry patches. Dry patches causes reduction in heat transfer coefficient and sometimes the failure of the tubes also occurs. On the other hand, vertical plate falling film evaporators are more compact, cheaper, lower fouling resistance and higher heat transfer coefficient than that of the shell and tube configuration [2, 3, 7].

Tube geometry and tube size have an important role on the performance of the falling film evaporators. Geometry of the tube can be varied by enhancing techniques (thermal spray metallic coating, creating grooves on the tube surface etc.) and also by changing the shape of the tube. Enhancing the tube can provide better heat transfer coefficient mainly because of increase in the number of nucleation sites, increase in the total surface area and the presence of turbulence [13]. A number of experimental studies [2, 6, 7, 11] have been reported in the literature about the enhancement techniques. Luo *et al.* [10] reported a better heat transfer performance by using non- circular tubes like oval shaped and drop shaped tubes and also reported a lower dimensionless temperature and a thinner thermal boundary layer.

Corrugated vertical plate evaporators are developing technology in the vertical plate evaporators category. Most of the published falling film studies concern laminar and turbulent fluid flow over a horizontal tube or over a flat vertical plate compared to corrugated vertical plate. Gonda *et al.* [6] conducted an experimental study on falling film evaporation over a corrugated vertical plate. Around 50% increase in Nusselts number is obtained compared to

smooth tube. And also Gonda *et al.* [6] reported that the flow regime is turbulent due to corrugated structure of the plate. The previous work which is somewhat related to vertical corrugated plate is by Kafi *et al.* [7]. Their studies are based on the evaporation of saline water over vertical smooth plate with horizontal metallic wires embedded on it. They reported high wetting, stability and turbulent falling film due to metallic wires on the plates.

Thermal spray metal coating is a heat transfer enhancement technique, which is done by spraying molten metal on any heat transfer surface. Studies by Abraham and Mani [1] shows that, compared to plain tubes, the performance of thermal spray metal coated tubes are 75-150% higher. Studies by Mohammad *et al.* [11] shows that the metal coating on plain tubes increases the heat transfer coefficient up to particular value, after that increase in coating thickness will decrease the value of heat transfer coefficient.

In the present study, a numerical model is developed for falling film evaporation over a thermal spray metal coated corrugated conduit. Fresh water is taken for the present computational study. A comparative study has been carried out between corrugated conduit and the circular tube.

2. COMPUTATIONAL METHODS

2.1 Physical and Computational Domain

The component which is more interested in the present study is vertical corrugated plate conduits shown in figure 1(a). It is made up of two stainless steel plates which are deformed to get sinusoidal corrugations on plates and welded together by horizontal rods to get conduits. The test section consists of a re-distributor and the corrugated conduits. As the name implies, the main function of re-distributor is to distribute the water to the corrugated conduits.

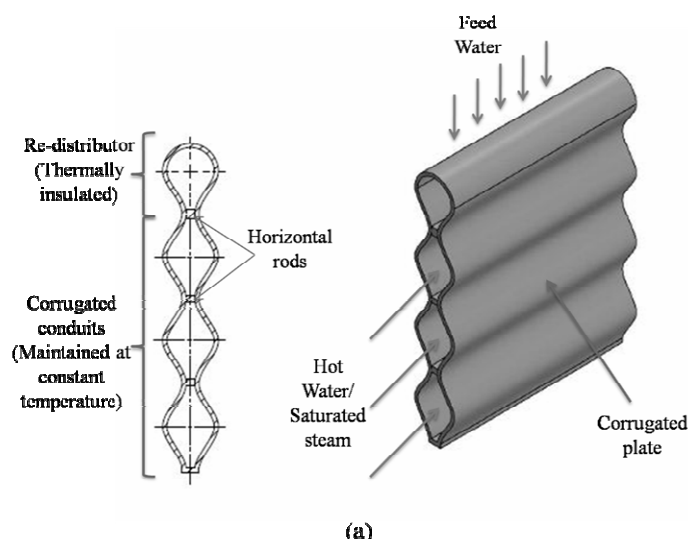


Figure 1(a): Physical structure of a vertical corrugated conduit

Figure 1(b) shows the computational domain used for the present study with boundary conditions. Re-distributor is thermally insulated. The length L is taken as 33 mm, amplitude A is taken as 10.7 mm and feeder height H is taken as 4 mm. Finite volume method based commercial software is used to carry out the heat transfer studies on falling film evaporation on corrugated plate.

2.2 Governing Equations

Pressure based solver is employed in the present model. For turbulence modeling $k-\omega$ turbulence model with shear stress transport (SST) is used. $k-\omega$ is well suited for simulations inside the viscous sub-layer and $k-\epsilon$ is well suited for simulations away from the wall. So, this ensures that appropriate equation is used throughout the flow field. For interface tracking, volume of fluid (VOF) method is used. Compressive scheme is used for the discretization of volume fraction equation. The VOF solves two sets of continuity equations for liquid and vapour phase and a single set of momentum and energy equations for combined phase of liquid and vapour.

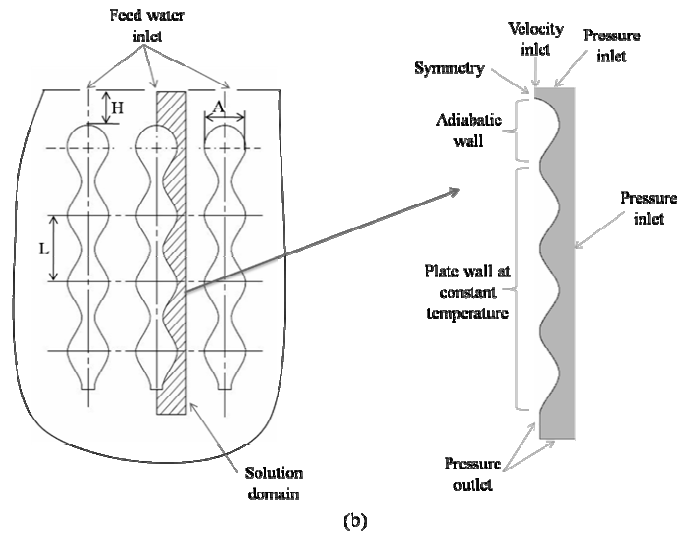


Figure 1(b): Computational domain with boundary conditions for the present model

$$\frac{\partial}{\partial t}(\alpha_f \rho_f) + \nabla \cdot (\alpha_f \rho_f \bar{u}_f) = S_f \quad (1)$$

$$\frac{\partial}{\partial t}(\alpha_g \rho_g) + \nabla \cdot (\alpha_g \rho_g \bar{u}_g) = S_g \quad (2)$$

$$\frac{\partial}{\partial t}(\rho \bar{u}) + \nabla \cdot (\rho \bar{u} \bar{u}) = -\nabla p + \nabla \cdot \left[\mu (\nabla \bar{u} + \nabla \bar{u}^T) \right] + \rho \bar{g} + \bar{F} \quad (3)$$

$$\frac{\partial}{\partial t}(\rho E) + \nabla \cdot (\bar{u}(\rho E + P)) = \nabla \cdot (k_{eff} \nabla T) + S_e \quad (4)$$

$$E = \frac{\alpha_f \rho_f E_f + \alpha_g \rho_g E_g}{\alpha_f \rho_f + \alpha_g \rho_g} \quad (5)$$

$$\rho = \alpha_f \rho_f + \alpha_g \rho_g \quad (6)$$

$$\mu = \alpha_f \mu_f + \alpha_g \mu_g \quad (7)$$

$$k_{eff} = \alpha_f k_f + \alpha_g k_g \quad (8)$$

2.3 Phase change Model

The main challenge of simulation of two-phase flow is considering the heat and mass transfer during phase change. Several phase change models are proposed in literature. The commonly used phase change models for evaporation and condensation are based on model by Lee [15] and model by Tanasawa [16]. From literatures [5, 8, 14] reported that interfacial temperature obtained by means of Lee and Tanasawa numerical technique will not be exactly the saturation temperature. The empirical constants used in Lee model and in the Tanasawa model does not have any physical limits. Therefore, excessively small values of these empirical constants lead to a significant deviation between interfacial and saturation temperature. However, too large values cause convergence problems and therefore optimal values must be found.

Third phase change model, which is used in the present study, is called sharp interface model, which uses the Rankine – Hugoniot jump condition for energy conservation at the interface. This model is purely theoretical and does not depend upon any empirical constants. The interfacial heat flux jump and mass flux can be calculated by using equations (9) and (10) respectively.

$$q_i'' = -k_{eff} (\nabla T_i \cdot \vec{n}) \quad (9)$$

$$\dot{m}'' = \frac{-k_{eff} (\nabla T_i \cdot \vec{n})}{h_{fg}} \quad (10)$$

Mass and energy source terms calculated from sharp interface model is given in equations (11) and (12) respectively.

$$S_g = -S_f = \dot{m}'' |\nabla \alpha_g| = \frac{k_{eff} (\nabla \alpha_g \cdot \nabla T)}{h_{fg}} \quad (11)$$

$$S_e = S_f h_{fg} \quad (12)$$

2.4 Grid and Time-step size

Mesh and time independence studies are carried out. The mesh size used for the present model is 140336. Boundary layer meshing method is used and a y^+ value of less than 5 is taken for the calculation of first layer thickness. Structured mesh is used for the entire domain. The convergence criteria used for the present model is 10^{-6} for energy equation and 10^{-4} for both continuity and momentum equation. The time step used for the present study is 10^{-4} s.

3. RESULTS AND DISCUSSION

3.1 Heat Transfer Coefficient

For the calculation of local film evaporative heat transfer coefficient, value of wall heat flux is calculated at various locations after a steady film is formed and equation (13) is used to calculate the local film heat transfer coefficient. For finding the average heat transfer coefficient area weighted average of wall heat flux is calculated and is given in the equation (14). Equation (15) and (16) give the average film heat transfer coefficient and average Nusselt number respectively.

$$h(x) = \frac{q_w(x)}{T_w - T_{sat}} = \frac{-k_f \frac{\partial T}{\partial y} \Big|_{y=0}}{T_w - T_{sat}} \quad (13)$$

$$\overline{q_w} = \frac{\int_0^L q(x) dA_s}{\int_0^L dA_s} \quad (14)$$

$$\overline{h} = \frac{\overline{q_w}}{T_w - T_{sat}} \quad (15)$$

$$\overline{Nu}_u = \frac{\overline{h}}{k_f} \left[\frac{\mu_f^2}{\rho_f^2 g} \right]^{1/3} \quad (16)$$

In order to validate the present numerical solution an experimental study by Gonda *et al.* [6] from literature is selected. Geometry shape, dimensions (L= 22.7mm and A= 5mm) and the operating conditions except the heating method are same as that of the experimental studies. The dimensions above mentioned are used only for validation of the present numerical model. L= 33mm and A= 10.7mm are used for the remaining parametric study. Figure (2)

shows the comparison of present study with experimental results by Gonda *et al.* [6]. From the results, at higher Reynolds numbers, the current numerical results are in good agreement with the deviation of 16%.

Figure (3) shows the comparison of present numerical study, with no surface roughness, about film evaporation over the corrugated conduit with the results of film evaporation over smooth tube from literature. It is clear from the graph is that an enhancement in heat transfer is observed for corrugated conduit. At least 50% enhancement in heat transfer is observed by comparing the present results with results by Chun and Seban [4]. At lower Reynolds numbers the performance of corrugated conduit is poor compared to Parken *et al.* [12]. But it is found that the overall values of heat transfer coefficient are higher for corrugated conduit compared to circular tube. It is mainly due to the following reasons. Firstly, the effective contact area between the corrugated conduit and the liquid film is larger. Secondly, the liquid film is turbulent because of the sinusoidal shape of the corrugated conduit.

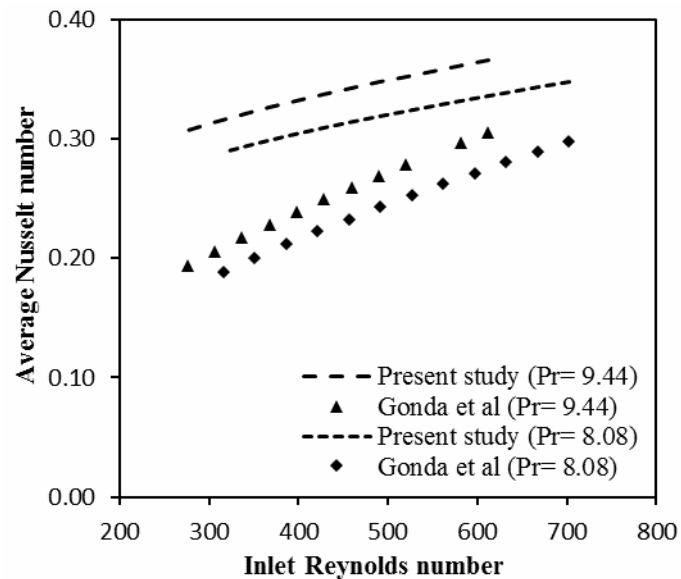


Figure 2: Comparison of present results with the literature for vertical corrugated conduit

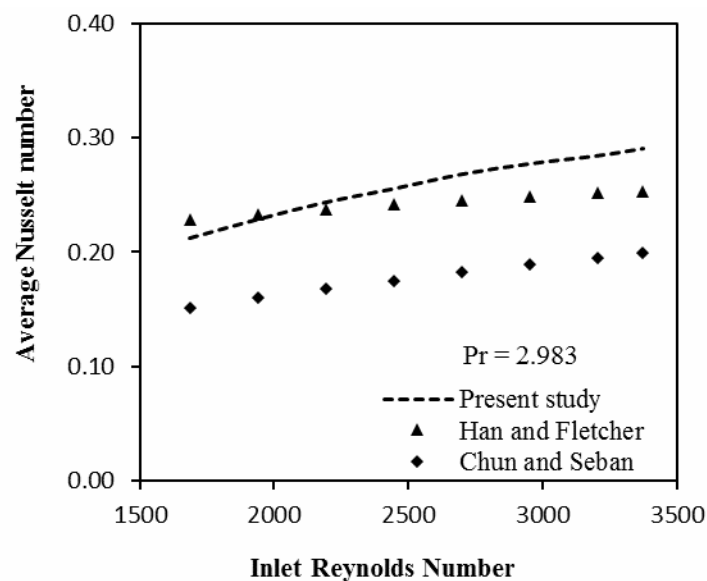


Figure 3: Comparison of present results with literature on falling film evaporation over tubes

From Jacobi *et al.* [12] under fully conventional conditions, the heat transfer coefficient is increasing with increase in flow rate. Figure (4) shows the variation of heat transfer coefficient with inlet Reynolds number for two Prandtl numbers. Heat transfer coefficient is increases with Reynolds number and not very appreciably with Prandtl number.

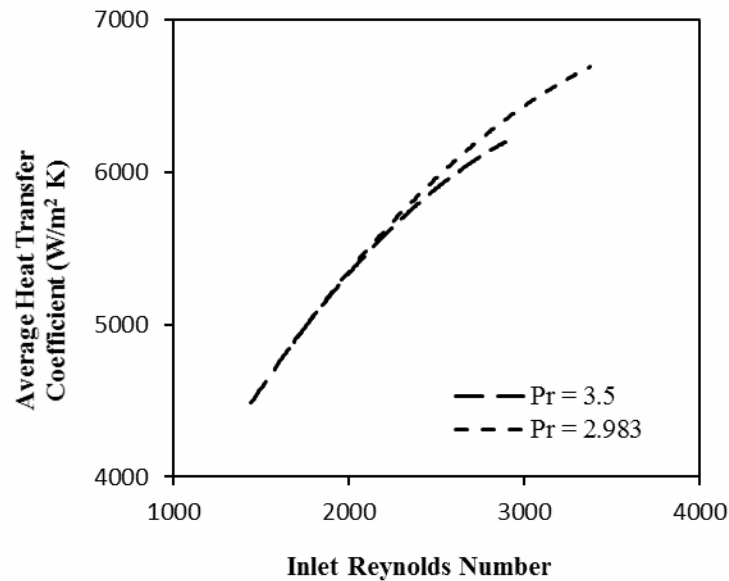


Figure 4: Variation of average heat transfer coefficient with inlet Re

Conventional heat transfer coefficient is directly depends upon the fluid velocity. So increase in flow rate causes increase in fluid velocity that lead to increase in heat transfer coefficient. Figure (5) shows the variation of local heat transfer coefficient along the surface. Local heat transfer coefficient decreases from the top of the surface until at a particular location for all flow rates and then tend to have a relatively uniform distribution with periodic fluctuations as the flow approaches the bottom of the surface.

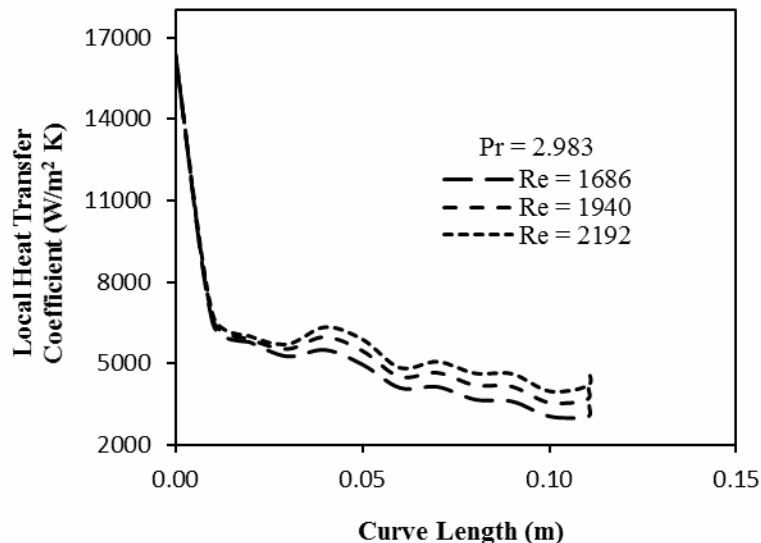


Figure 4: Variation of heat transfer coefficient along the surface

For the present study, a wall super heat of 3K is used. From the Fig. (6), there is no systematic variation of the heat transfer coefficient is observed. So the heat transfer coefficients are almost independent of wall superheat for fully conventional (without boiling phenomenon) conditions.

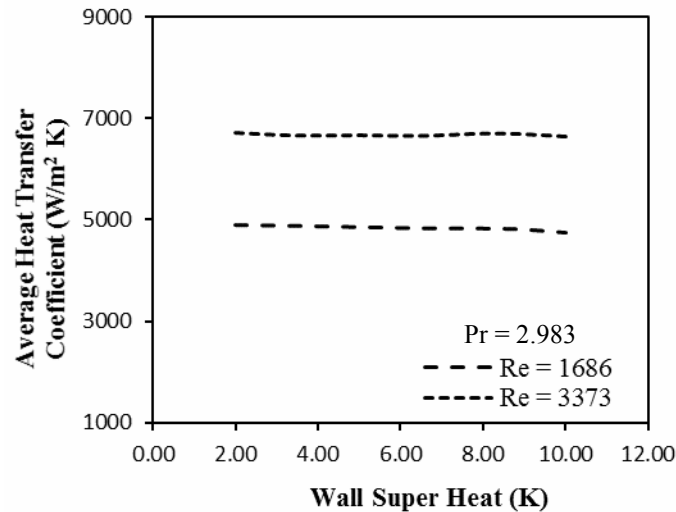


Figure 6: Variation of heat transfer coefficient with wall super heat

3.5 Effect of Surface Roughness on Heat Transfer Coefficient

Thermal spray metal coating is a heat transfer enhancement technique, by increasing the roughness of the surface, which is done by spraying molten metal on any heat transfer surface. Surface roughness plays a major role in heat transfer enhancement by increasing the turbulence effects as well as by providing higher wetting compared to plain surfaces. Figure 7(a) shows the variation of heat transfer coefficient with surface roughness. It is clear from the figure that, the increase in heat transfer coefficient with surface roughness is very less. It is mainly because of the roughness heights which are in the order of 10^{-6} m. The same phenomenon is also reported in studies by Abraham and Mani [1]. Figure 7(b) shows the variation of heat transfer coefficient with inlet Reynolds number for both coated and non-coated surface. At lower Reynolds number the heat transfer coefficient for both the surfaces are almost same, but at higher heat transfer coefficient an observable difference of 3.3% is noticed.

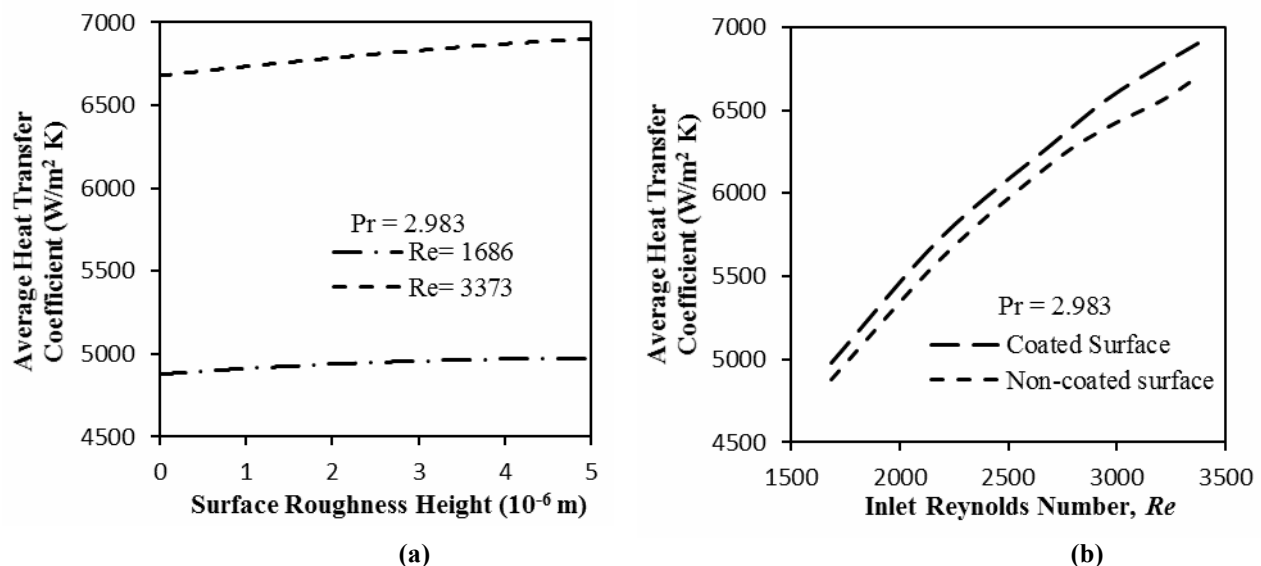


Figure 6: (a) shows the variation of heat transfer coefficient with roughness height and (b) shows the comparison of heat transfer coefficient of coated and non-coated surface

3.6 Temperature Profile

Figure (8) shows the non-dimensional temperature profiles across the liquid film at five different axial locations for $Re = 2891$ and $Pr = 3.5$. Using the phase change model, the interface temperature is managed to maintain at saturation temperature with a maximum error of $\pm 0.5^{\circ}C$.

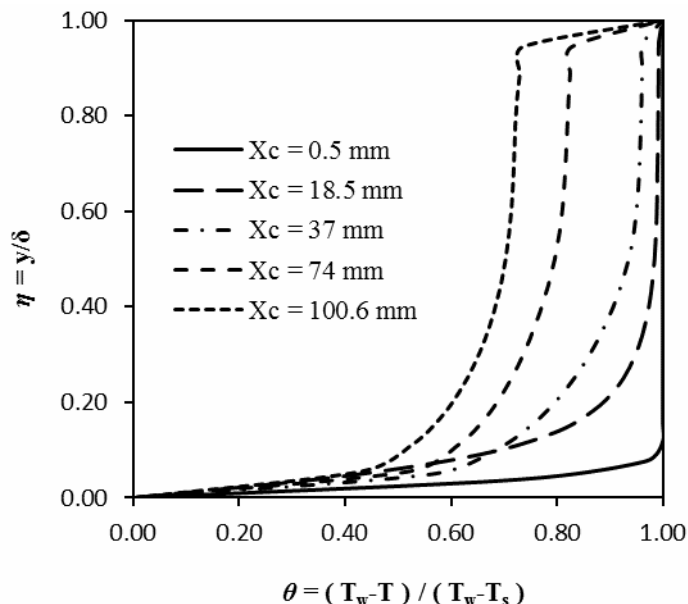


Figure 8: Non-dimensional temperature profile at different curve lengths (X_c)

At smaller curve lengths, the temperature gradient at the interface is very small. So the large amount of heat flux given at the wall is used to heat the liquid film itself and the evaporation rate is also small. Liquid film is thermally developing at the interface at curve lengths (X_c) of 0.5 mm, 18.5 mm, and 37 mm. But for larger curve lengths 74 mm and 100.6 mm a steep temperature gradients can be seen at both wall and at the interface. An appreciable amount of heat flux will be dissipating at the interface. Therefore the evaporation rate is also higher at these regions. So we can say that the film is almost thermally fully developed at the interface.

4. CONCLUSIONS

The present numerical study examined heat transfer characteristics of falling film evaporation over a corrugated conduit. Conclusions are arrived at based on the numerical studies as follows:

- Heat transfer across the interface is successfully captured with the aid of the sharp interface phase change model. And the interface is managed to maintain at saturation temperature with a maximum deviation of $\pm 0.5^\circ\text{C}$.
- The liquid film heat transfer coefficient of corrugated plate conduit is at least 15% higher than that of circular tube at higher Reynolds numbers.

NOMENCLATURE

E	Energy per unit mass	(J/kg)
g	Acceleration due to gravity	(m/s ²)
h	Heat transfer coefficient	(W/m ² K)
h_{fg}	Latent heat of vaporization	(J/kg)
k	Thermal conductivity	(W/m K)
Pr	Prandtl number	$(\mu_f c_{p,f} / k_f)$
p	Pressure	(N/m ²)
q_w	Wall heat flux	(W/m ²)
Re	Reynolds number	$(4\Gamma / \mu_f)$
S	Volumetric mass source term	(kg/m ³ s)
T	Temperature	(K)
X_c	Curve length	(m)
y^+	Dimensionless distance perpendicular to the wall	$(y u^* / \nu_f)$

y Distance perpendicular to the wall. (m)

Greek symbols

ρ Density
 μ Dynamic viscosity
 Γ Mass flow rate per unit length
 δ Film thickness
 θ Dimensionless temperature
 η Dimensionless film thickness

Subscript

eff Effective
 e Energy
 f Liquid
 g Vapour
 sat Saturation
 tur Turbulent
 w Wall

REFERENCES

1. Abraham, R. & Mani, A. (2013). Effect of flame spray coating on falling film evaporation for multi-effect distillation system. *Desalination and Water Treatment*, 51(4-6), 822-829.
2. Abraham, R. & Mani, A. (2015). Experimental studies on thermal spray-coated horizontal tubes for falling film evaporation in multi-effect desalination system. *Desalination and Water Treatment*, 56(1), 71-82.
3. Abraham, R. & Mani, A. (2015). Heat transfer characteristics in horizontal tube bundles for falling film evaporation in multi-effect desalination system. *Desalination*, 375(), 129-137.
4. Chun, K. R. & Seban, R. A. (1971). Heat Transfer to Evaporating Liquid Films. *J. Heat Transfer*, 93(4), 391-396.
5. De Schepper, S. C. K., Heynderickx, G. J. & Marin, G. B. (2009). Modeling the evaporation of a hydrocarbon feedstock in the convection section of a steam cracker. *Computers and Chemical Engineering*, 33(), 122-132.
6. Gonda, A., Lancereau, P., Bandelier, L., Luo, L., Fan, Y. & Benezech, S. (2014). Water falling film evaporation on a corrugated plate. *International Journal of Thermal Sciences*, 81(), 29-37.
7. Kafi, F., Renaudin, V., Alonso, D. & Hornut, J. M. (2004). New med plate desalination process: thermal performances. *Desalination*, 166 (), 53-62.
8. Kharangate, C. R., Lee, H. & Mundawar, I. (2015). Computational modeling of turbulent evaporating falling films. *International Journal of Heat and Mass Transfer*, 81(), 52-62.
9. Kouhikamal, R., Noori Rahim Abadi, S. M. A. & Hassani, M. (2014). Numerical investigation of falling film evaporation of multi-effect desalination plant. *Applied Thermal Engineering*, 70(), 477-485.
10. Luo, L., Zhang, G., Pan, J. & Tian, M. (2013). Flow and heat transfer characteristics of falling water film on horizontal circular and non-circular cylinders. *Journal of Hydrodynamics*, 25(), 404-414.
11. Mohammad Siraj Alam., Prasad, L., Gupta, S. C. & Agarwal, V. K. (2008). Enhanced boiling of saturated water on copper coated heating tubes. *Chemical Engineering and Processing*, 47(1), 159-167.
12. Parken, W. H., Fletcher, L. S., Sermas, V. & Han, J. C. (1990). Heat transfer through falling film evaporation and boiling on horizontal tubes. *Trans. ASME*, 112 (), 744-750.
13. Ribatski, G. & Jacobi, A. M. (2005). Falling film evaporation on horizontal tubes-a critical review. *International Journal of Refrigeration*, 28(), 635-653.
14. Sun, D., Xu, J. & Chen, Q. (2014). Modeling of the Evaporation and Condensation Phase-Change Problems with FLUENT. *Numerical Heat Transfer*, 66(), 326-342.
15. Lee, W. H. (1980). A pressure iteration scheme for two-phase flow modeling. In: T.N. Veziroglu (Ed.), *Multiphase Transport Fundamentals, Reactor Safety, Applications*. Washington, DC: Hemisphere Publishing.
16. Tanasawa, I. (1991). Advances in condensation heat transfer. In J. P. Hartnett & T. F. Irvine (Eds.), *Advances in Heat Transfer*. San Diego, CA: Academic Press.